Medical Physics
The International Journal of Medical Physics Research and Practice

Monte Carlo calculations of electron beam quality conversion factors for several ion chamber types

B. R. Muir and D. W. O. Rogers

Citation: Medical Physics **41**, 111701 (2014); doi: 10.1118/1.4893915
View online: http://dx.doi.org/10.1118/1.4893915
View Table of Contents: http://scitation.aip.org/content/aapm/journal/medphys/41/11?ver=pdfcov
Published by the American Association of Physicists in Medicine

Monte Carlo calculations of electron beam quality conversion factors for several ion chamber types

B. R. Muir[a)]
Measurement Science and Standards, National Research Council Canada, 1200 Montreal Road, Ottawa, Ontario K1A 0R6, Canada

D. W. O. Rogers[b)]
Carleton Laboratory for Radiotherapy Physics, Physics Department, Carleton University, 1125 Colonel By Drive, Ottawa, Ontario K1S 5B6, Canada

(Received 3 March 2014; revised 23 June 2014; accepted for publication 13 August 2014; published 7 October 2014)

Purpose: To provide a comprehensive investigation of electron beam reference dosimetry using Monte Carlo simulations of the response of 10 plane-parallel and 18 cylindrical ion chamber types. Specific emphasis is placed on the determination of the optimal shift of the chambers' effective point of measurement (EPOM) and beam quality conversion factors.
Methods: The EGSnrc system is used for calculations of the absorbed dose to gas in ion chamber models and the absorbed dose to water as a function of depth in a water phantom on which cobalt-60 and several electron beam source models are incident. The optimal EPOM shifts of the ion chambers are determined by comparing calculations of R_{50} converted from I_{50} (calculated using ion chamber simulations in phantom) to R_{50} calculated using simulations of the absorbed dose to water vs depth in water. Beam quality conversion factors are determined as the calculated ratio of the absorbed dose to water to the absorbed dose to air in the ion chamber at the reference depth in a cobalt-60 beam to that in electron beams.
Results: For most plane-parallel chambers, the optimal EPOM shift is inside of the active cavity but different from the shift determined with water-equivalent scaling of the front window of the chamber. These optimal shifts for plane-parallel chambers also reduce the scatter of beam quality conversion factors, k_Q, as a function of R_{50}. The optimal shift of cylindrical chambers is found to be less than the 0.5 r_{cav} recommended by current dosimetry protocols. In most cases, the values of the optimal shift are close to 0.3 r_{cav}. Values of k_{ecal} are calculated and compared to those from the TG-51 protocol and differences are explained using accurate individual correction factors for a subset of ion chambers investigated. High-precision fits to beam quality conversion factors normalized to unity in a beam with $R_{50} = 7.5$ cm (k'_Q) are provided. These factors avoid the use of gradient correction factors as used in the TG-51 protocol although a chamber dependent optimal shift in the EPOM is required when using plane-parallel chambers while no shift is needed with cylindrical chambers. The sensitivity of these results to parameters used to model the ion chambers is discussed and the uncertainty related to the practical use of these results is evaluated.
Conclusions: These results will prove useful as electron beam reference dosimetry protocols are being updated. The analysis of this work indicates that cylindrical ion chambers may be appropriate for use in low-energy electron beams but measurements are required to characterize their use in these beams.
 [http://dx.doi.org/10.1118/1.4893915]

Key words: electron beam reference dosimetry, EGSnrc, k_Q, k_{ecal}, beam quality conversion factors, EPOM, dosimetry protocols

1. INTRODUCTION

The calibration of clinical treatment machine output is prescribed by reference dosimetry protocols,[1,2] which are based on ion chambers calibrated in a cobalt-60 reference field. Cobalt-60 ion chamber calibrations are traceable to national standards for absorbed dose. The beam quality conversion factor, k_Q, is required to convert the cobalt-60 absorbed dose to water calibration coefficient, $N^{Co}_{D,w}$, with the reading of the ion chamber, M, in the clinical beam to the quantity of interest, the absorbed dose to water, D_w, in the clinical beam of interest with

$$D_w = MN^Q_{D,w} = k_Q MN^{Co}_{D,w}. \quad (1)$$

For electron beams, the determination of k_Q factors recommended in current dosimetry protocols required some assumptions (e.g., that the wall correction factor was unity in electron beams) and, in some cases, used data available at the time that had high systematic uncertainties. The individual correction factors on which the protocol k_Q factors are based have been shown to be up to 1.7% different compared to more accurate Monte Carlo calculations.[3] There is current

interest in updating clinical reference dosimetry protocols and recent publications have provided accurate measured and Monte Carlo calculated k_Q factors, but results have mostly been obtained for photon beams.[4–10] A small number of publications[11–13] have focused on the determination of electron beam k_Q factors but only for a few chamber types.

Reference dosimetry protocols recommend the use of plane-parallel chambers for low-energy electron beams ($E_0 < 10$ MeV), but the stability of plane-parallel chamber calibrations have been shown to be questionable.[9,14] Due to the potentially problematic behavior of plane-parallel chambers, it may be more appropriate to use stable cylindrical ion chambers for electron beam reference dosimetry, even for low-energy beams. Consequently, there is interest in characterizing the use of cylindrical chambers for electron beam reference dosimetry. Plane-parallel chambers can still be used for clinical reference dosimetry if they are cross-calibrated against stable cylindrical chambers each time they are used or if they have been shown to be stable enough to be considered as reference-class detectors. Therefore, there is still interest in obtaining accurate k_Q factors for plane-parallel chambers. The focus of this work is on the determination of electron beam quality conversion factors for several of the plane-parallel and cylindrical ion chambers available on the market today. In addition, the use of an effective point of measurement (EPOM) and how gradient effects are accounted for when accurately determining dosimetric quantities, such as the beam quality specifier and beam quality conversion factors, are important issues for electron beam reference dosimetry that are investigated here.

2. METHODS

In our recent publication,[13] an in-depth investigation into electron beam reference dosimetry was presented using Monte Carlo simulations as a function of depth with the plane-parallel PTW Roos and cylindrical NE2571 ion chamber models. In the present work, the same approach is followed using 10 plane-parallel and 18 cylindrical ion chamber models and a review of the method appears here but the reader is referred to our previous work[13] for more details.

2.A. Beam quality conversion factors

Beam quality conversion factors, k_Q, have been calculated in previous publications[4–6,8–13] as the ratio of Monte Carlo calculations of the absorbed dose to water, D_w, to the absorbed dose to air in an ion chamber, D_{ch}, in an electron beam with quality Q to that in cobalt-60

$$k_Q = \left(\frac{D_w}{D_{ch}}\right)^{Q}_{Co}. \tag{2}$$

This equation requires that $(W/e)_{air}$, the mean energy deposited in air per coulomb of charge released by electrons slowing in air be equal in cobalt-60 and in electron beams of quality Q. It was recently shown that $(W/e)_{air}$ varies by at most 0.36% (95% confidence) in radiation therapy beams up to 25 MV relative to its value in ^{60}Co. However, the value of $(W/e)_{air}$ for cobalt-60 and MV photon beams is for an entire slowing down spectrum of electrons. In contrast, $(W/e)_{air}$ for electron beams will be much closer to $(w/e)_{air}$, the energy deposited in the air in the active cavity of an ion chamber per coulomb of charge released by electrons of a certain energy, since the electrons crossing the air in the chamber at d_{ref} will be much closer to monoenergetic. Early estimates involving $(w/e)_{air}$ in electron beams suggested that $(w/e)_{air}$ might vary by up to 1.5% over the entire range of clinically relevant electron energies[15] although the experimental results used for this analysis had 1% measurement uncertainties and relied on the use of stopping-power ratios for monoenergetic electrons, not the realistic spectrum of electrons that would be present for the measurements. A more recent reanalysis of the same data reports no variation at the 0.4% level.[16]

2.B. Monte Carlo calculations as a function of depth

Instead of performing the calculations required for Eq. (2) at only the reference depth as in most other publications, D_w and D_{ch} are calculated as a function of depth in a water phantom. We recently showed[13] that if R_{50}, the depth at which the absorbed dose to water falls to 50% of its maximum value, is determined with D_w calculations as a function of depth, the results are different from those obtained by calculating I_{50} using simulations of D_{ch} as a function of depth and converting to R_{50} using the equation recommended by TG-51 ($R_{50} = 1.029 I_{50} - 0.063$ cm).[1] This equation is based on the results of Ding *et al.*[17] who used simulations of absorbed dose to water and water-to-air stopping-power ratios to find the relationship between I_{50} and R_{50} and therefore assumes a perturbation-free ion chamber. However, after correcting the depth-ionization data calculated with the NE2571 and PTW Roos chamber models by using the Ding *et al.*[17] conversion from I_{50} to R_{50}, optimal shifts of the depth-dose data enable more accurate determination of R_{50}. Optimal shifts for accurate R_{50} determination are investigated for all ion chambers here by determining the shift which minimizes the difference between R_{50} calculated from water and chamber simulations for 24 beams ranging from 4 to 22 MeV.

With calculations of D_w and D_{ch} as a function of depth, k_Q factors are extracted at the reference depth ($d_{ref} = 0.6R_{50} - 0.1$cm) using Eq. (2). Simple linear fitting of the data is used to reduce statistical fluctuations in D_w/D_{ch} ratios. In addition, gradient effects are investigated for cylindrical chambers using calculations of D_{ch} vs depth.

Recall that in TG-51,[1] the electron beam k_Q factor is factored with

$$k_Q = P^Q_{gr} k_{R_{50}}, \tag{3}$$

where P^Q_{gr} corrects for gradient effects and $k_{R_{50}}$ is the component of k_Q that is independent of gradient effects. Calculations of $k_{R_{50}}$ provided in TG-51 were calculated as

$$k_{R_{50}} = \frac{\left[\left(\frac{\bar{L}}{\rho}\right)^{water}_{air} P_{cel} P_{fl} P_{wall}\right]^{Q}}{\left[\left(\frac{\bar{L}}{\rho}\right)^{water}_{air} P_{cel} P_{repl} P_{wall}\right]^{Co}}, \tag{4}$$

where, in the notation of the AAPM, the effect of the chamber's central electrode is corrected with P_{cel}, the effect of the chamber's wall is corrected with P_{wall} and $P_{repl} = P_{fl}P_{gr}^{Q}$ corrects for the effect of the air cavity causing changes in the electron spectrum. Notice that in the numerator, only the fluence correction factor is included such that, by definition, $k_{R_{50}}$ does not include gradient effects for electron beams.

For well-guarded plane-parallel chambers, the gradient correction was taken to be unity for TG-51 with the point of measurement at the front of the active cavity. In our previous paper,[13] we noted that the use of $k_{R_{50}}$ implies that a gradient correction is required to obtain $k_{R_{50}}$ from k_Q calculations. As in TG-51, we do not use P_{gr}^{Q} for plane-parallel chambers so we just refer to k_Q for these chamber types. However, we investigate the use of an EPOM on k_Q. In practice, the use of an EPOM introduces an effective chamber perturbation correction by accounting for gradient effects and other perturbations caused by the ion chamber (e.g., the effects of chamber walls). We previously[13] found that using the optimal EPOM shift described above to position the PTW Roos chamber for calculations of k_Q factors reduced the scatter of k_Q as a function of R_{50}. We will show that the same is true for the plane-parallel chambers investigated in this work (see Sec. 3.C)

For cylindrical chambers, TG-51 recommended a clinically measured gradient correction

$$P_{gr}^{Q} = \frac{M(d_{ref} + 0.5\ r_{cav})}{M(d_{ref})}, \tag{5}$$

where P_{gr}^{Q} is obtained as the ratio of the ion chamber reading, M, at a depth of $d_{ref} + 0.5\, r_{cav}$ (r_{cav} is the radius of the air cavity of the cylindrical chamber) to that at the reference depth. We previously[13] calculated the gradient correction with

$$P_{gr}^{Q} = \frac{D_{ch}(d_{ref} + f\ r_{cav})}{D_{ch}(d_{ref})}, \tag{6}$$

i.e., P_{gr}^{Q} is calculated as the ratio of D_{ch} at $d_{ref} + f\ r_{cav}$ to that at d_{ref}, where f is a fraction of the cavity radius. The fraction f was then varied to obtain the optimal gradient correction to reduce the root-mean-square deviation (RMSD) of a fit to $k_{R_{50}}$ vs R_{50}. However, for the NE2571 chamber, we found[13] that if only clinical beams were considered, the scatter in k_Q factors as a function of R_{50} (i.e., intrinsically including gradient effects by definition rather than using P_{gr}^{Q} to obtain $k_{R_{50}}$) was low enough for accurate reference dosimetry. The same analysis is performed here for other cylindrical chambers.

2.C. Calculations of k_{ecal} and $k'_{R_{50}}$

The TG-51 protocol factors $k_{R_{50}}$ using the photon–electron conversion factor, k_{ecal}, and the electron quality conversion factor, $k'_{R_{50}}$, via

$$k_{R_{50}} = k_{ecal} k'_{R_{50}} \equiv k_{R_{50},ecal} k'_{R_{50}}. \tag{7}$$

The k_{ecal} factor is fixed for a given chamber type and is simply $k_{R_{50}}$ for an electron beam of quality Q_{ecal} with $R_{50} = 7.5$ cm

$$k_{ecal} \equiv k_{R_{50},ecal} = k_{R_{50}=7.5\ cm} = \frac{k_Q(R_{50} = 7.5\ cm)}{P_{gr}^{Q}}. \tag{8}$$

The subscript R_{50} in $k_{R_{50}}$ implies that an explicit gradient correction has not been included in this factor. Since we investigate the use of both $k_{R_{50}}$ (where a gradient correction has been calculated and removed from k_Q) and k_Q (which includes gradient effects intrinsically by definition), it is useful at this point to introduce new notation. We make use of the notation $k_{R_{50}}$, $k'_{R_{50}}$ and $k_{R_{50},ecal}$, which are used in the same manner as in TG-51 and exclude gradient effects [Eqs. (3), (7), and (8)]. In contrast, the analogous factors obtained using calculated k_Q factors (which do not require an explicit P_{gr}^{Q} but include gradient effects by definition) are represented by k_Q, k'_Q and $k_{Q,ecal}$, such that

$$k'_Q = k_Q / k_{Q,ecal}, \qquad k_{Q,ecal} \equiv k_Q(R_{50} = 7.5\ cm), \tag{9}$$

for both plane-parallel and cylindrical chambers.

For all calculations of $k_{R_{50},ecal}$ or $k_{Q,ecal}$ in this work, a fit to the $k_{R_{50}}$ or k_Q data as a function of R_{50} is made to extract the value of $k_{R_{50}}$ or k_Q at $R_{50} = 7.5$ cm. There are, however, different ways that the $k_{R_{50}}$ or k_Q calculations are performed. For plane-parallel chambers, k_Q is calculated with the reference depth at the inside of the chamber window (i.e., the front of the air cavity) using the physical window thickness for comparison to TG-51 calculations. Calculations of k_Q are also performed with the optimal EPOM for accurate R_{50} determination which also serve to reduce the scatter of k_Q as a function of R_{50}.

For cylindrical chambers, there are three ways to determine $k_{R_{50}}$ or k_Q factors. For comparison to TG-51, $k_{R_{50}}$ is calculated after dividing k_Q by P_{gr}^{Q} determined from Eq. (6) with $f = 0.5$. Another method is to divide k_Q by P_{gr}^{Q} determined using the optimal shift to calculate $k_{R_{50}}$. Finally, if only clinical beams are considered, a reasonable approach is to consider k_Q (where the gradient correction is included in k_Q and no explicit correction for gradient effects is needed). As with plane-parallel chamber calculations, a fit to $k_{R_{50}}$ or k_Q vs R_{50} is made and $k_{R_{50},ecal}$ or $k_{Q,ecal}$ is extracted at $R_{50} = 7.5$ cm.

2.D. Simulation geometry and ion chamber models

The EGSnrc (Refs. 18 and 19) user-code egs_chamber (Ref. 20) is used for all simulations to calculate absorbed dose. Calculations are obtained as a function of depth close to the surface of a $30 \times 30 \times 30$ cm^3 water phantom on which beams are incident to depths well into the bremsstrahlung tail. The absorbed dose to air, D_w, is calculated in disks of water with radii of 0.5 cm and thicknesses between 0.05 and 0.2 cm depending on the incident beam energy. Similarly, the absorbed dose to the gas in fully modeled ion chambers, D_{ch}, is calculated as the chambers are translated through the phantom with step sizes between 0.05 and 0.2 cm depending on the incident beam energy. Temporary phase-space scoring in an artificial geometry that encloses the chamber model at

all depths of interest is used to increase the efficiency of these simulations.[20]

EGSnrc Monte Carlo transport parameters are set to their defaults except for the use of NIST bremsstrahlung cross-sections. For simulations of absorbed dose in electron beams, electron and photon cutoff energies and production thresholds are set to 521 and 10 keV, respectively. They are set to 512 and 1 keV, respectively, for cobalt-60 simulations. We did not observe[13] differences outside of statistical uncertainties in electron beam simulations with reduced electron and photon cutoff energies and production thresholds.

The ion chamber models used here are the same as those described in our previous publications.[8,9,21] Simulations are performed for all plane-parallel chambers investigated previously:[9]

PTW—Roos, Markus, and Advanced Markus;
IBA—NACP-02, PPC-40, and PPC-05; and
Exradin—A10, A11, P11, and P11TW.

There is still some uncertainty about the correct density of graphite in the front window of the IBA NACP-02 chamber; so calculations are performed for this chamber with graphite densities of both 1.7 g/cm^3, as recommended by the manufacturer and 2.25 g/cm^3, as suggested by Chin *et al.*[22]

Only the subset of cylindrical chambers that are considered to be reference-class detectors,[7,23] based on measurements in photon beams, are used for the calculations of this work:

NE—2571 and 2611;
PTW—30010, 30011, 30012, 30013, and 31013;
IBA—FC65G, FC65P, FC23C, CC25, and CC13;
Exradin—A12, A19, A12S, A18, and A1SL; and
Capintec—PR06C/G.

2.E. Source models

All sources in this work are modeled at a source-to-surface distance (SSD) of 100 cm collimated to a field size of 10×10 cm^2 at the surface of the phantom. Cobalt-60 simulations use the photon spectrum of Mora *et al.*,[24] but in our previous work,[13] differences were not observed outside of statistical uncertainties of 0.05% when using different models to simulate the cobalt-60 source when the calculations used 1 (512) keV cutoff energies and production thresholds for photons (electrons).

Based on our previous results,[13] representative clinical linear accelerators as well as electron beams which are not representative of clinical treatment machines are selected for source simulation in this work. The nonclinical accelerator beams are the discontinued AECL Therac-20 accelerator, Vickers research linac and beams shaped with the discontinued Type II applicator for the Varian Clinac accelerator. Table I provides the electron beams used here with calculated R_{50} values and the percentage bremsstrahlung tail. All sources with $R_{50}>6.5$ cm and all of the Elekta *Precise* accelerator beams are simulated with BEAMnrc (Ref. 25) and subsequently used as a shared library input to egs_chamber simulations. BEAMnrc accelerator simulations are used for sources with $R_{50}>6.5$ cm because of the influence of contaminant photons on the D_w/D_{ch} ratio from high-energy beams observed previously.[13] All of the Elekta *Precise* accelerator beams, regardless of incident energy, are modeled using BEAMnrc to ensure that significant differences are not present compared to simulations that use electron beam spectra for any of the chambers investigated. The BEAMnrc accelerator simulations use 10 (700) keV cutoff energies and production thresholds for photons (electrons). All other electron beams with $R_{50}<6.5$ cm are modeled as collimated point sources from the electron beam spectra of Ding and Rogers.[26] The interested reader is referred to our previous work[13] where the electron beam models used here are described in more detail.

TABLE I. Characteristics of the electron beam models used for source simulation. Except for the Elekta Precise accelerator, which was modeled for this work (see text), the source of the BEAMnrc accelerator model is indicated beside the accelerator name. All electron beam spectra are obtained from Ding and Rogers (Ref. 26) and used to model a 10×10 cm^2 point source incident on the surface of the phantom. Beams that are considered to be typical of current clinical accelerators are in italics.

Accelerator	Nominal energy (MeV)	R_{50} (cm)	Bremsstrahlung tail % of D_{max}
BEAMnrc accelerator models			
Elekta Precise	4	1.79	0.36
	8	3.29	1.18
	12	4.93	2.03
	18	7.04	3.00
	22	8.73	4.94
Varian Clinac 2100C[a]	18	7.72	3.78
Siemens KD2[b]	21	8.32	4.82
Electron beam spectra			
Varian Clinac 2100C[c]	6	2.64	0.13
	9	4.02	0.31
Varian Clinac 2100C[d]	6	2.66	0.14
	9	4.12	0.33
Varian Clinac 2100C[c]	12	5.19	0.48
	15	6.49	0.57
Siemens KD2	6	2.31	0.12
	11	4.21	0.34
Elekta SL25	4	1.69	0.05
	8	2.80	0.15
Elekta SL75-5	5	2.11	0.09
	10	4.15	0.33
	14	6.03	0.68
AECL Therac-20	6	2.22	0.09
	9	3.44	0.23
	13	5.18	0.48
NRC Vickers	10	3.97	0.30

[a]Accelerator model from Rogers *et al.* (Ref. 27) (Type II applicator).
[b]Accelerator model from Ding and Rogers (Ref. 26).
[c]Spectra from Ding and Rogers (Ref. 26) (Type II applicator).
[d]Spectra from Ding and Rogers (Ref. 26) (Type III applicator).

TABLE II. Different possible locations of the EPOM shift from the front surface of the front window of plane-parallel chambers. The physical thickness of the chamber window (used by TG-51) is shown along with the water equivalent (g/cm^2) window thickness (suggested in TRS-398) and the optimal shift for R_{50} determination from I_{50} calculations. The statistical uncertainty in the optimal shift is less than 0.04 mm for all chambers. Column 6 is the optimal EPOM shift from the front of the cavity (i.e., from the inside of the front window). Two different models of the IBA NACP-02 chamber are provided that use different graphite densities in the front window of the chamber. Chambers that require a water-proofing cap for use in water include a cap in the model used for calculations and are indicated by an asterisk.

Manufacturer	Chamber	Physical thickness (mm)	Water-equivalent scaling (mm)	Optimal shift (mm)	Shift into cavity (mm)
PTW	Roos	1.13	1.34	1.55	0.42
	Markus*	1.27	1.06	1.54	0.27
	Advanced Markus*	1.27	1.06	1.24	−0.03
IBA	NACP-02				
	(1.7 g/cm^3)	0.60	0.99	1.13	0.53
	(2.25 g/cm^3)	0.60	1.26	1.31	0.71
	PPC-40	1.00	1.24	1.39	0.39
	PPC-05	1.00	1.76	1.58	0.58
Exradin	A10*	1.04	1.25	1.48	0.44
	A11	0.99	1.74	1.77	0.78
	P11	0.99	1.15	1.40	0.41
	P11TW*	1.04	1.25	1.66	0.62

TABLE III. Offsets upstream from the central axis giving the EPOM for accurate R_{50} determination with cylindrical chambers. The statistical uncertainty in the optimal shift for accurate R_{50} determination is less than 0.05 mm (between 0.01 and 0.02 r_{cav}, depending on the cavity radius) for all chambers.

Manufacturer	Chamber	r_{cav} (mm)	Δz as a fraction of r_{cav} for R_{50} determination
NE	2571[a]	3.14	0.33
	2611[b]	3.70	0.24
Exradin[c]	A12	3.04	0.35
	A19	3.00	0.34
	A12S	3.04	0.37
	A18	2.43	0.18
	A1SL	2.01	0.11
PTW	30010	3.05	0.33
	30011	3.05	0.31
	30012	3.05	0.31
	30013	3.05	0.38
	31013	2.75	0.35
IBA	FC65G	3.10	0.35
	FC65P	3.10	0.37
	FC23C	3.10	0.29
	CC25	3.00	0.29
	CC13	3.00	0.23
Capintec	PR06C/G	3.22	0.31

[a]Manufactured by Elektron Technology.
[b]Manufactured by NPL.
[c]Manufactured by Standard Imaging.

3. RESULTS AND DISCUSSION

3.A. Optimal shifts for R_{50} determination

Table II provides different possibilities for positioning plane-parallel chambers. The shifts given in Table II are from the front face of the chamber window (i.e., if the physical shift is used to position the chamber, the EPOM is at the inside of the front window of the plane-parallel chamber or the front of the active cavity). Table II provides the physical thickness of the front window of the chamber, which is recommended by TG-51 (Ref. 1) for positioning of plane-parallel chambers. Also shown is the water-equivalent shift of the chamber, determined with water-equivalent scaling of the front window using the physical density and physical thickness of the window as recommended by the IAEA TRS-398 protocol[2] for positioning plane-parallel chambers. Due to the small difference between the physical and water-equivalent thicknesses, the TRS-398 protocol[2] indicates on p. 44 that this difference may be neglected in practice.

Table II also shows the optimal EPOM shift calculated here to accurately determine R_{50} using plane-parallel chambers. The EPOM for the Advanced Markus chamber is shifted by a small amount into the air gap between the front window/collector and the water-proofing cap. For all other plane-parallel chambers, the EPOM is shifted into the air cavity. Similarly, Table III provides optimal shifts for R_{50} determination for cylindrical chambers as a fraction of the cavity radius as well as the cavity radius. The EPOM for all cylindrical chambers is shifted upstream from the center of the cavity toward the radiation source.

In our previous work,[13] we showed that using a shift of the chamber allows for more accurate R_{50} determination with conversion from I_{50} because it reduces the variation of the overall ion chamber perturbation factor, P_Q, with depth. In this work, the optimal shift to minimize the variation of P_Q with depth is tested for a sample of ion chambers (the plane-parallel IBA NACP-02 chambers with both window densities, the Exradin A10 and A11 chambers and the cylindrical IBA FC65G, the Exradin A12 and the PTW 31013 chambers) and the results confirm that the required shift is similar to that for accurate R_{50} determination shown in Tables II and III. Details on how this optimization is performed are in our previous work.[13] Also note that in our previous work,[13] beam energy-dependent shifts were required to minimize the variation of P_Q with depth, whereas the values in Tables II and III are the optimal shifts for R_{50} determination combining results from all beams investigated. We recommend the practical use of these optimal EPOM shifts because their use improves the accuracy of electron beam reference dosimetry in the sense that they allow for more accurate determination of R_{50} and reduce the scatter of calculated k_Q factors as a function of R_{50} (see Sec. 3.C) without complicating the procedure used for reference dosimetry (i.e., by requiring beam energy-dependent ion chamber shifts).

3.B. Comparison of recommended shifts to literature data

The shifts that optimize R_{50} determination for plane-parallel chambers are different from those recommended for chamber positioning in current reference dosimetry protocols[1,2] and indicate that the EPOM should be shifted inside the chamber cavity for most chambers. Lacroix *et al.*[28] explained that the use of water-equivalent scaling of the chambers' front window for positioning plane-parallel chambers is equivalent to applying a first-order perturbation correction. That the shifts determined here are different from those calculated using water-equivalent scaling of the front window of the chamber suggests that factors other than the front window are being accounted for with the use of the optimal shift (e.g., contributions to D_{ch} from the side and back walls or the influence of the air cavity).

3.B.1. Comparison to previous measurements

For cylindrical chambers, the TG-51 and IAEA TRS-398 protocols recommend the use of a 0.5 r_{cav} upstream shift for chamber positioning based on the measured results of Johansson *et al.*[29] from 1977. When measured results are used to determine the EPOM shift for ion chambers, some standard must be selected. Johansson *et al.*[29] assumed that the EPOM for the NACP chamber was correct and compared depth-ionization results measured with cylindrical chambers and the NACP standard to deduce the suggested upstream shift of 0.5 r_{cav} for cylindrical chambers. It is unclear whether the NACP chamber window was scaled for water-equivalence for chamber positioning. As in Johansson *et al.*,[29] Van der Plaetsen *et al.*[30] compared depth-ionization data measured with an NE2571 chamber to that from their NACP standard (positioned with the EPOM at the inner surface of the window without water-equivalent scaling) to determine shifts between 0.3 r_{cav} and 0.6 r_{cav} in low- and high-energy electron beams, respectively. In our calculations, if the EPOM of the NACP chamber is taken as the inside of the front window (without scaling) the difference between the NACP EPOM and the optimal EPOM for the NE2571 in Table III is 0.5 r_{cav} and slightly different if the EPOM is found with water-equivalent scaling of the NACP front window (0.6 r_{cav}). These results are in good agreement with the measured differences of Johansson *et al.*[29] and Van der Plaetsen *et al.*,[30] especially given that the measurements rely on the accuracy of chamber positioning as well as the assumed shift for the selected standard used for comparison.

In this work, the optimal shift for R_{50} determination using cylindrical ion chambers is still upstream but for all chambers investigated is less than the 0.5 r_{cav} recommended in current reference dosimetry protocols.[1,2] The shift is close to 0.3 r_{cav} for most chambers but is as small as 0.11 r_{cav} for the Exradin A1SL chamber, which has a comparatively smaller volume. Recommendations for such small shifts call into question the level of positioning uncertainty achievable in modern radiotherapy clinics. The required shift for R_{50} determination with the cylindrical chambers investigated is less than 1.2 mm. For the Exradin A1SL chamber, the required shift is only 0.2 mm and it is doubtful that modern radiotherapy clinics can—or should be required to—achieve this level of precision when positioning ion chambers.

Roos *et al.*[31] compared depth–ionization data from Markus chambers to that determined using Roos and NACP standards when chamber positioning used water-equivalent scaling of the chambers' front window. The difference in the shift determined for the Markus chamber was between 0.5 and 0.6 mm, independent of whether the Roos or NACP standard was used. The difference between the water equivalent EPOM for the Roos (NACP) chamber and the optimal EPOM of the Markus chamber is 0.2 mm (0.55 mm), in reasonable agreement with the results of Roos *et al.*[31] More recently, Lacroix *et al.*[28] compared measurements from PTW Roos and NACP-02 chambers as a function of depth to those from a plastic scintillating detector, their assumed perturbation-free standard, to determine the EPOM for the plane-parallel chambers. In 6, 12, and 18 MeV beams, respectively, their results amount to 1.12 ± 0.1, 1.4 ± 0.1, and 1.9 ± 0.2 mm for the PTW Roos chamber and 1.0 ± 0.1, 1.25 ± 0.1, and 1.8 ± 0.2 mm for the NACP-02 chamber. Their results are similar to the optimal shifts in Table II of 1.55 mm for the PTW Roos chamber and 1.13 or 1.31 mm (depending on the assumed window density) for the NACP-02 chamber. However, in this work, results for all beams are combined instead of performing a separate analysis for different beams, in which case beam energy-dependent shifts are observed[13] as seen in the experiments.

3.B.2. Comparison to previous calculations

Unlike the procedure used to obtain measured EPOMs, Monte Carlo calculated values do not require that a standard be selected for comparison. However, calculated EPOMs are sensitive to the specifications and materials of the ion chamber model used for the calculations, as noted earlier[32] as well as in our previous publication.[13] If these models are not representative of the ion chambers being used for clinical measurements, potential errors are possible if the use of a shift is recommended using values based on Monte Carlo calculations. In Sec. 3.E, we discuss the sensitivity of our calculated results to the specifications used to create ion chamber models. In what follows, we compare the calculated EPOM shifts obtained here with those obtained by other authors using Monte Carlo simulations of ion chamber response in electron beams.[32–34] Since the results of this work and all previous Monte Carlo calculated EPOM shifts used the EGSnrc code system, there is some correlation among the results discussed in this comparison.

Zink and Wulff[33] investigated the issue of the EPOM for the PTW Roos chamber by varying the shift of the chamber's EPOM to minimize the variation of the overall ion chamber perturbation factor with depth in 6, 11, and 21 MeV beams. Their results amount to 1.48 ± 0.03, 1.51 ± 0.05 and 1.51 ± 0.05 mm in 6, 11, and 21 MeV beams, respectively, in good agreement with the 1.55 mm value in Table II. In the same publication, Zink and Wulff[33] studied the variation of the wall correction factor for the PTW Roos chamber with depth and observed that a beam energy independent EPOM shift into the

chamber cavity by 0.17 mm minimizes the variation of P_{wall} with depth which compares to our value of 0.42 mm in Table II.

In a subsequent publication,[34] the same authors found that the use of an EPOM shift of 0.58 mm from the inside of the front face into the NACP-02 chamber cavity minimizes the variation of P_{wall} with depth. The model used in that work is based on the publication of Chin *et al.*[22] who suggested that the mass thickness of the front wall of the NACP-02 chamber should be increased by about 50%. The result of Zink and Wulff[34] is similar to the corresponding value of 0.71 mm in Table II although the results of the present work also account for the effect of the air cavity on the electron fluence.

Wang and Rogers[32] studied the issue of the EPOM including different components of ion chambers for various chamber types. When considering a wall-less cavity, they observed that the shift to minimize the variation of the chamber perturbation factor (in this case the replacement correction factor, P_{repl}) was 0.18 mm downstream for the PTW Roos chamber, 0.45 mm downstream for the PTW Markus chamber, 0.25 mm downstream for the NACP-02 chamber and 0.51 r_{cav} or 0.41 r_{cav} for the NE2571 chamber in 22 or 6 MeV beams. If one adds the results that separately minimize the variation of the P_{wall} (Refs. 33 and 34) and P_{repl} (Ref. 32) correction factors with depth along with the physical thickness of the front windows of the chambers, the results are 1.48 mm for the PTW Roos chamber and 1.43 mm for the NACP-02 chamber. These are similar to the results from Table II, if one compares to the result obtained here with increased graphite density in the front window of the NACP-02 chamber.

Wang and Rogers[32] also investigated the shift to minimize the variation of the overall chamber perturbation, P_Q, with depth using full ion chamber models. For the NE2571 chamber (albeit using a chamber model without a water-proofing sleeve unlike the one used here that includes a sleeve), the required shifts are 0.46 r_{cav} and 0.33 r_{cav} in 22 and 6 MeV beams, respectively, in reasonable agreement with the result of 0.33 r_{cav} from Table III. For the standard model of the NACP-02 chamber ($\rho_g = 1.7$ g/cm^3), Wang and Rogers[32] observed that shifts of 0.7 and 0.5 mm downstream from the front of the cavity were necessary to minimize the variation of P_Q with depth in 22 and 6 MeV beams compared to 0.53 mm here when results from all beams are combined to obtain the optimal shift for accurate R_{50} determination. When they increased the thickness of the graphite and MYLAR in the NACP-02 front window by 50% (comparable to the calculation here that uses $\rho_g = 2.25$ g/cm^3), the results were 0.8 and 0.65 mm in the same beam energies. This is in good agreement with the result of 0.71 mm from Table II. Finally, they[32] found that the variation of P_Q with depth for a PTW Markus chamber could be minimized with shifts of 0.15 and 0.2 mm in 22 and 6 MeV beams, in reasonable agreement with the value of 0.27 mm from Table II.

To conclude this section, there have been several publications including our previous paper[13] that investigate the issue of the EPOM in electron beams and find shifts that depend on beam quality. The EPOM shifts presented here are for the accurate determination of R_{50} using ion chambers, combining results from all beams investigated. These shifts also serve to reduce the scatter of calculated k_Q factors as a function of R_{50} for plane-parallel chambers (Ref. 13 and below). Overall, these results are in good agreement with the data from the literature but are different from recommendations in current dosimetry protocols.

3.C. Beam quality conversion factors for plane-parallel chambers

3.C.1. $k_{Q,ecal}$

Table IV provides calculated $k_{Q,ecal}$ factors [Eq. (9)] for plane-parallel chambers when the optimal EPOM is used or, for comparison to TG-51, when the EPOM is at the front of the chamber cavity. Differences between calculated $k_{Q,ecal}$ values are not significant for plane-parallel chambers using different shifts; the difference, comparing the values obtained using the optimal shift described above and that using the TG-51 recommendation, is at most 0.3% for the Exradin A11 and IBA PPC-05, which may not be significant given the amount of scatter present in the calculated k_Q factors as a

TABLE IV. The photon–electron conversion factor, $k_{Q,ecal}$, [Eq. (9)] for plane-parallel chambers. Values are provided using the optimal EPOM shift determined here for R_{50} determination (Table II, column 5) and when the front of the cavity (i.e., the inside of the front window) is used as the EPOM shift to compare to TG-51 values.

		$k_{Q,ecal}$			
Manufacturer	Chamber	Optimal EPOM	Physical EPOM	TG-51	Difference (%)
PTW	Roos	0.898	0.899	0.901	−0.20
	Markus	0.898	0.899	0.905	−0.71
	Advanced Markus	0.899	0.899		
IBA	NACP-02 (1.7 g/cm^3)	0.892	0.893	0.888	0.61
	NACP-02 (2.25 g/cm^3)	0.894	0.896		
	PPC-40	0.900	0.901		
	PPC-05	0.890	0.893		
Exradin	A10	0.923	0.924		
	A11	0.906	0.909		
	P11	0.883	0.885	0.888	−0.36
	P11TW	0.879	0.881		

TABLE V. Exponential fitting parameters for plane-parallel chambers for k'_Q as a function of R_{50} for a fit of the form given in Eq. (10). The EPOM used is that which optimizes R_{50} determination.

		Exponential fitting parameters			
Manufacturer	Chamber	a	b	c	RMSD (%)
PTW	Roos	0.984	0.134	3.511	0.11
	Markus	0.984	0.112	3.826	0.10
	Advanced Markus	0.986	0.135	3.349	0.11
IBA	NACP-02 (1.7 g/cm^3)	0.985	0.135	3.398	0.10
	NACP-02 (2.25 g/cm^3)	0.983	0.135	3.649	0.12
	PPC-40	0.985	0.130	3.510	0.12
	PPC-05	0.982	0.104	4.248	0.14
Exradin	A10	0.991	0.113	2.927	0.13
	A11	0.992	0.114	2.864	0.13
	P11	0.989	0.177	2.687	0.12
	P11TW	0.990	0.165	2.720	0.15

function of R_{50} when the TG-51 recommendation is used to define the EPOM (RMSD = 0.3% for both chambers).

We previously[13] explained the differences between the calculated $k_{Q,\text{ecal}}$ factors for the PTW Roos chamber [Eq. (9)] and those of TG-51 by applying the corresponding TG-51 $k_{Q,\text{ecal}}$ equations [like Eq. (4), normalized to unity in a beam with $R_{50} = 7.5$ cm] but with more accurate Monte Carlo calculations of the individual correction factors. Although differences between the individual Monte Carlo calculated correction factors and those used for TG-51 calculations are up to 0.6%, the $k_{Q,\text{ecal}}$ factors are within 0.2% for the Roos chamber (also shown in Table IV). We noted[13] that accurate Monte Carlo calculated stopping-power ratios are very close to those used for TG-51 $k_{Q,\text{ecal}}$ calculations. Of the three other plane-parallel chambers that overlap between this study and TG-51, literature data for individual correction factors are available for two chambers allowing a comparison between this work and TG-51. Given the small differences in stopping-power ratios, only the wall and replacement correction factors need to be considered. The calculated $k_{Q,\text{ecal}}$ factor for the IBA NACP-02 chamber is 0.6% different from the TG-51 recommended value. The P_{repl} factor was assumed to be unity for TG-51 $k_{Q,\text{ecal}}$ calculations in both cobalt-60 and in high-energy electron beams ($R_{50} = 7.5$ cm). Monte Carlo simulations determine that P_{repl} factors for the NACP-02 chamber are 1.0063 (Ref. 35) (^{60}Co) and 1.0005 (Refs. 12, 35, and 36) ($R_{50} = 7.5$ cm). For TG-51 k_{ecal} calculations, the P_{wall} factor in cobalt-60 for the NACP-02 chamber was taken to be 1.018 based on EGS4 simulations,[37] and unity in high-energy electron beams. More recent Monte Carlo simulations confirm that P_{wall} is 1.0207 in ^{60}Co (Refs. 3 and 38) and at R_{50} = 7.5 cm is between 1.0060 (Ref. 12) and 1.0086 (Ref. 3). The difference between the calculated k_{ecal} factor for the NACP-02 chamber from this work and that from TG-51 is therefore mostly due to differences in the ^{60}Co P_{repl} factors and differences in the P_{wall} factors in high-energy electron beams.

The calculated $k_{Q,\text{ecal}}$ factor for the PTW Markus chamber in Table IV is 0.7% different from that provided in TG-51. Monte Carlo calculations of P_{repl} are 0.997 (Refs. 12 and 36) in a high-energy electron beam ($R_{50} = 7.5$ cm) and 1.0055 (Ref. 12) in cobalt-60 compared to the values of 0.998 ($R_{50} = 7.5$ cm) and unity (^{60}Co) used for TG-51 calculations. Meanwhile, the Monte Carlo calculated P_{wall} factor is 1.005 (Refs. 3 and 12) ($R_{50} = 7.5$ cm), whereas TG-51 assumed that P_{wall} was unity for ion chambers in high-energy electron beams. The calculated P_{wall} factors are 1.005 (Refs. 3 and 38) or 1.0066 (Ref. 12) for the Markus chamber in cobalt-60 compared to the value of 0.998 used by TG-51. Therefore, the difference in the calculated $k_{Q,\text{ecal}}$ factor for the Markus chamber calculated here compared to that of TG-51 results from differences in $P^{\text{Co}}_{\text{repl}}$ and P_{wall} values in both beam qualities.

3.C.2. k'_Q

Fits to k'_Q calculations [Eq. (9)] vs R_{50} are made for all plane-parallel chambers with

$$k'_Q = a + b \times e^{-R_{50}/c} \tag{10}$$

when the optimal EPOM for accurate R_{50} determination is used. We previously[13] showed that using this optimal EPOM also reduces the RMSD of a fit to calculated k'_Q factors for the PTW Roos chamber. The worst RMSD of the fit to the data here is only 0.15% for all plane-parallel chambers investigated, comparable to the statistical uncertainty on the calculated k'_Q values. Table V provides the fitting parameters for plane-parallel chambers.

In Fig. 1(a), k'_Q calculations are presented as a function of R_{50} for the PTW Roos chamber and the two models of the NACP-02 chamber when the optimal EPOM shift for accurate R_{50} determination is used. Different shifts of plane-parallel chambers do not produce large effects on k'_Q or $k_{Q,\text{ecal}}$ calculations. Differences in k'_Q are less than 0.3% in very low-energy beams when the optimal shift or physical shift is used. Table IV shows less than 0.3% differences in $k_{Q,\text{ecal}}$ factors when different shifts are used for positioning plane-parallel chambers. Figure 1(a) also shows the negligible difference in k'_Q calculations vs R_{50} (i.e., energy dependence of k_Q normalized to the results from high-energy beams with $R_{50} = 7.5$ cm) between the three chamber models.

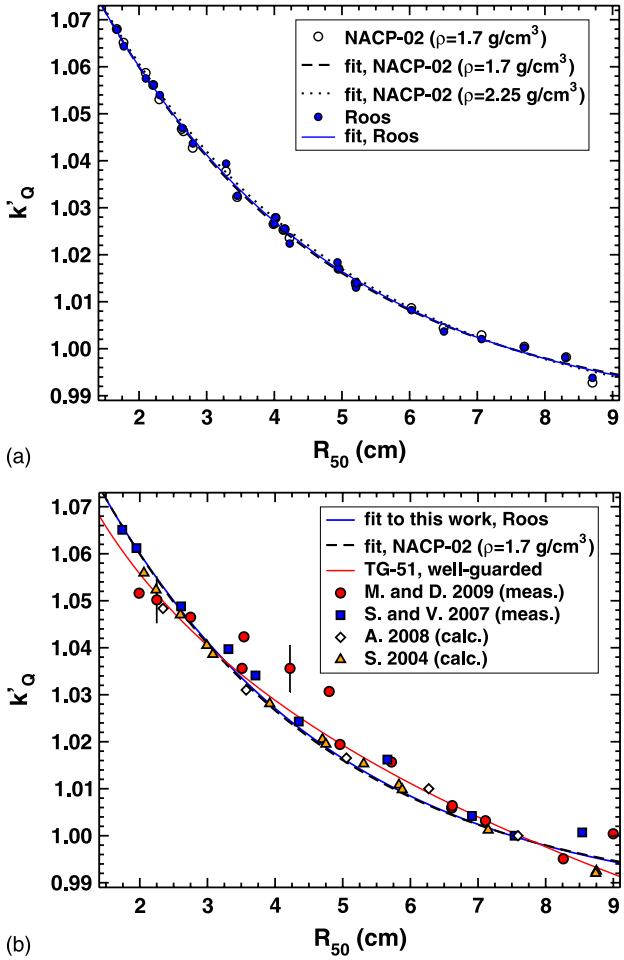

FIG. 1. The electron quality conversion factor, k'_Q for the plane-parallel PTW Roos and IBA NACP-02 chambers. (a) Calculations of this work for different chamber types. Simulated results that use different graphite densities in the front window of the NACP-02 chamber are shown. The optimal shift for accurate R_{50} determination is used for positioning the chambers but the trend of k'_Q is not significantly affected when different shifts are used. Statistical uncertainties on the calculations are less than 0.1%. (b) Comparison of the calculations of this work to literature values including the fit from the TG-51 protocol (Ref. 1) for well-guarded plane-parallel chambers, the compiled measured data from McEwen and DuSautoy (Ref. 39), the measured data of Stucki and Voros (Ref. 40), the calculated data of Araki (Ref. 41), and the calculated results of Sempau *et al.* (Ref. 42). Representative error bars are shown for a few of the measured data points from McEwen and DuSautoy (Ref. 39).

Figure 1(b) shows the fit to calculated k'_Q obtained here for the IBA NACP-02 and PTW Roos chambers compared to values from the literature. The k'_Q calculations are at most 0.4% different from the fit as a function of R_{50} provided by TG-51 for well-guarded plane-parallel chambers. McEwen and DuSautoy[39] compiled measured data for PTW Roos and IBA NACP-02 chamber types from water calorimetry measurements performed at McGill University and the National Research Council of Canada (NRC) and graphite calorimetry measurements performed at the National Physical Laboratory (NPL). The measurement uncertainties in these values are on the order of 0.4%. Stucki and Voros[40] measured k'_Q values for Roos and NACP-02 chambers using Fricke ferrous sulfate dosimetry with a measurement uncertainty of 0.5%. The measured results are in good agreement with the calculations of this work. These simulated values are also in good agreement with those of Araki,[41] who performed Monte Carlo calculations of (D_w/D_{ch}) in electron beams for the same chamber types. Those calculated results also used the EGSnrc (Refs. 18 and 19) Monte Carlo code system, albeit with independently modeled ion chambers and different source models. Finally, Sempau *et al.*[42] calculated (D_w/D_{ch}) in electron beams with an IBA NACP-02 chamber model using the PENELOPE code system. Overall, the normalized energy dependence observed here for the most commonly used plane-parallel chamber types is in excellent agreement with published data, giving confidence in these calculations.

Figure 2(a) shows k_Q calculations for the PTW Markus chamber compared to the calculated results of Zink and Wulff,[12] who used the same Monte Carlo code system as the present study but different source and ion chamber models. When the same EPOM (determined with water-equivalent scaling of the front window of the chamber) and model of

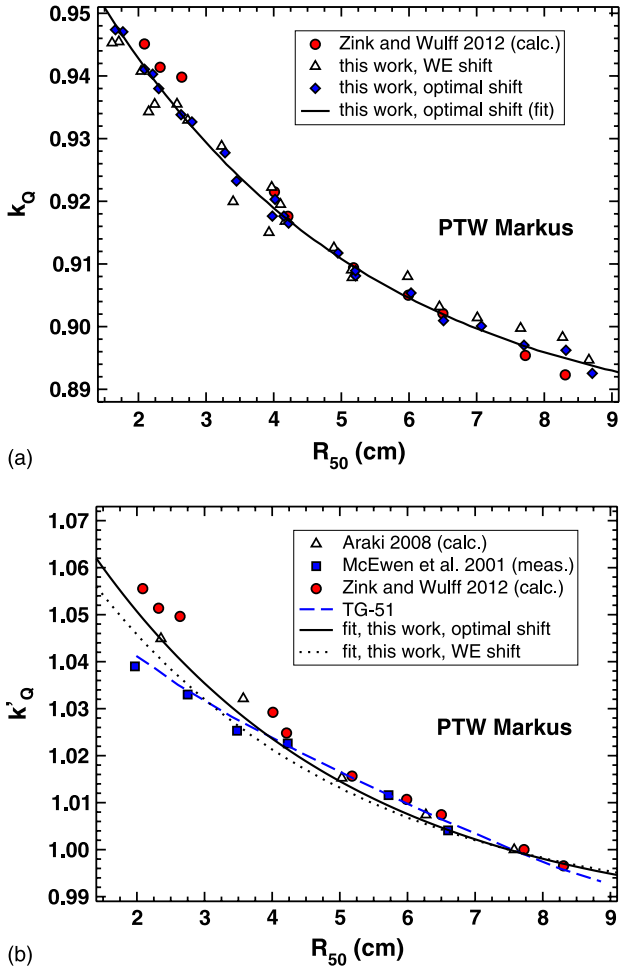

FIG. 2. Beam quality conversion factors for the PTW Markus chamber. (a) The effects on k_Q of using different shifts to position the chamber where WE refers to water-equivalent scaling of the front window of the chamber and the optimal shift is that for accurate R_{50} determination. The results of Zink and Wulff (Ref. 12) are shown for comparison (see discussion in the text). (b) Fits to the k'_Q data of this work as a function of R_{50} compared to calculated data from Zink and Wulff (Ref. 12), Araki (Ref. 41), the measured data of McEwen *et al.* (Ref. 43), and TG-51 (Ref. 1). Zink and Wulff and Araki used a water equivalent EPOM.

the PTW Markus chamber are used, the calculations of this work and those of Zink and Wulff[12] are in good agreement. Differences (up to 0.6%) between the results of this work in Fig. 2(a) and those of Zink and Wulff[12] in low-energy beams are consistent with minor differences among the ion chamber models (≈0.3% effects). The sensitivity of these results to ion chamber models is revisited in Sec. 3.E. As discussed previously,[13] the differences in high-energy beams are due to the use of realistic BEAMnrc electron beam models in this work which include photon contamination compared to the high-energy electron beam source models from electron beam spectra used by Zink and Wulff.[12]

The other important observation regarding Fig. 2(a) is the scatter of k_Q calculations as a function of R_{50} when different EPOM shifts are used. When the optimal shift described above is used to position the chamber, the results are less scattered as a function of R_{50} compared to when the water-equivalent shift is used (0.10% RMSD vs 0.23%). The PTW Markus chamber represents an extreme case since the water equivalent EPOM shift is inside the chamber window (due to the presence of the air gap) and 0.48 mm different from the optimal EPOM. However, this observation is still true to a lesser extent for all of the plane-parallel chambers investigated here. Our previous publication[13] investigated this issue in detail for the PTW Roos chamber.

Figure 2(b) shows k'_Q calculations as a function of R_{50} for the PTW Markus chamber with different EPOM shifts compared to the measured data of McEwen *et al.*[43] In that work, $N_{D,w}$ coefficients were determined in electron beams for the PTW Markus chamber (positioned using water-equivalent scaling of the chamber's front window) by comparing the chamber reading to the absorbed dose to water at the reference depth from graphite calorimetry measurements at NPL. To compare the k'_Q calculations of this work to those measurements, a linear fit to the $N_{D,w}$ coefficients as a function of R_{50} is made and used to normalize the results to the value at $R_{50} = 7.5$ cm. The estimated measurement uncertainties were 0.75% and there could be effects from chamber-to-chamber variation among Markus chambers, as pointed out in that publication[43] as well as by other authors when investigating plane-parallel calibration coefficients or beam quality conversion factors in electron beams.[14,40] Figure 2(b) also shows that the calculated results of Zink and Wulff[12] for the PTW Markus chamber are up to 1.2% different from the results obtained here when the same water equivalent EPOM shift is used (as discussed above) while the agreement with Araki[41] is better except near $R_{50} = 3.5$ cm where the scatter in our data is also large.

3.D. Beam quality conversion factors for cylindrical chambers

3.D.1. $k_{R_{50},ecal}$ and $k_{Q,ecal}$

Table VI provides calculated $k_{R_{50},\mathrm{ecal}}$ and $k_{Q,\mathrm{ecal}}$ factors of this work for cylindrical chambers when different shifts are

TABLE VI. The $k_{R_{50},\mathrm{ecal}}$ and $k_{Q,\mathrm{ecal}}$ factors [Eqs. (8) and (9)] for cylindrical chambers using different methods described in Sec. 2.C. TG-51 $k_{R_{50},\mathrm{ecal}}$ values are provided for comparison with the % difference [(1-col5/col6) × 100%] compared to the results of this work when the TG-51 recommended gradient correction is applied to obtain $k_{R_{50}}$. The results in column 3 are based on clinical beams only.

		$k_{Q,\mathrm{ecal}}$	$k_{R_{50},\mathrm{ecal}}$			
		No P_{gr}^{Q}	P_{gr}^{Q} used here			
Manufacturer	Chamber	Clinical beams	Optimal	TG-51	TG-51	Difference (%)
NE	2571	0.903	0.906	0.908	0.903	−0.60
	2611	0.896	0.899	0.903	0.904	0.16
Exradin	A12	0.907	0.909	0.912	0.906	−0.62
	A19	0.904	0.906	0.909		
	A12S	0.907	0.909	0.912		
	A18	0.914	0.915	0.919		
	A1SL	0.914	0.914	0.917	0.915[a]	−0.24
PTW	30010	0.904	0.906	0.910	0.897[b]	−1.46
	30011	0.901	0.903	0.907	0.900[c]	−0.79
	30012	0.908	0.910	0.914	0.905[d]	−1.02
	30013	0.901	0.904	0.908		
	31013	0.902	0.905	0.907	0.898[e]	−1.00
IBA	FC65G	0.904	0.907	0.910		
	FC65P	0.902	0.905	0.909		
	FC23C	0.904	0.906	0.910		
	CC25	0.904	0.906	0.911		
	CC13	0.904	0.906	0.911	0.904[f]	−0.78
Capintec	PR06C/G	0.906	0.908	0.913	0.900	−1.43

[a]Comparison to TG-51 value for the similar A1 chamber.
[b]Comparison to TG-51 value for the N30001 chamber, which it replaced.
[c]Comparison to TG-51 value for the N30002 chamber, which it replaced.
[d]Comparison to TG-51 value for the N30004 chamber, which it replaced.
[e]Comparison to TG-51 value for the N31003 chamber, which it replaced.
[f]Comparison to TG-51 value for the similar Wellhofer IC-10 chamber.

used to obtain and remove the gradient correction as described in Sec. 2.C. When the TG-51 recommendation is used to calculate P_{gr}^{Q}, the $k_{R_{50},ecal}$ results are between 0.2% and 1.5% different from the values provided in TG-51 depending on the ion chamber under consideration. In our previous publication,[13] the difference between the calculated $k_{R_{50},ecal}$ factor and that from TG-51 for the NE2571 chamber was explained using accurate Monte Carlo calculations of individual correction factors. We performed a similar analysis above for plane-parallel chambers. For clarity and brevity, the same exercise is only done for the PTW 30010 chamber which has the largest difference in $k_{R_{50},ecal}$ compared to TG-51.

Calculations of individual correction factors in cobalt-60 and a high-energy electron beam are used to calculate $k_{R_{50},ecal}$ with Eq. (4) for the PTW 30010 chamber. These calculations use the methods described in our previous publication.[13] These are in reasonable agreement with the wall correction factors of Buckley and Rogers[44] and the replacement correction factors calculated by Wang and Rogers.[32,35] The values of stopping-power ratio, P_{wall} and P_{cel} in cobalt-60 used by TG-51 to calculate $k_{R_{50},ecal}$ for this chamber are very close to those from Monte Carlo calculations. The main difference in individual correction factors results from values of P_{repl} and P_{stem} in cobalt-60, calculated with Monte Carlo simulations to be 0.996 and 0.997, respectively, whereas TG-51 used a value of 0.992 for P_{repl} and assumed that the stem correction was unity. In a high-energy electron beam, the Monte Carlo calculated P_{cel} factor and stopping-power ratio are very close to those used for TG-51 $k_{R_{50},ecal}$ factors but the accurate calculations of P_{fl}, P_{wall}, and P_{stem} are 0.985, 1.002, and 0.997 compared to the corresponding values of 0.978, 1.0, and 1.0 used for TG-51 $k_{R_{50},ecal}$ calculations. The difference between the $k_{R_{50},ecal}$ factor of this work and that from TG-51 (1.46%) for the PTW 30010 chamber is therefore mainly due to differences in P_{fl} values (0.7%) although smaller differences in other individual correction factors are also present. Another potential difference between these calculations and those provided by TG-51 is the requirement to account for a calculated P_{gr}^{Q} factor here, whereas the correction factor was simply omitted for TG-51 calculations. Wang and Rogers[45] showed that calculated P_{gr}^{Q} corrections depend on the method used for calculations.

3.D.2. $k'_{R_{50}}$ and k'_Q

Figure 3 shows calculated k'_Q factors for the cylindrical NE2571, Exradin A12 and A1SL chambers. These results are k_Q factors (without using an EPOM and including gradient effects by definition) normalized to the value of $k_{Q,ecal}$ extracted from the fit to k_Q as a function of R_{50} at $R_{50} = 7.5$ cm. For comparison, the compiled measured data for NE2571 and Exradin A12 chambers from McEwen and DuSautoy[39] are shown, based on measurements with calorimetric primary standards. Figure 3 shows that the energy dependence of NE2571 and Exradin A12 chambers is similar and is in good agreement with measured results. Only one measured data point, an outlying result, disagrees with the calculated fits by a value larger than the measurement uncertainty (0.4%).

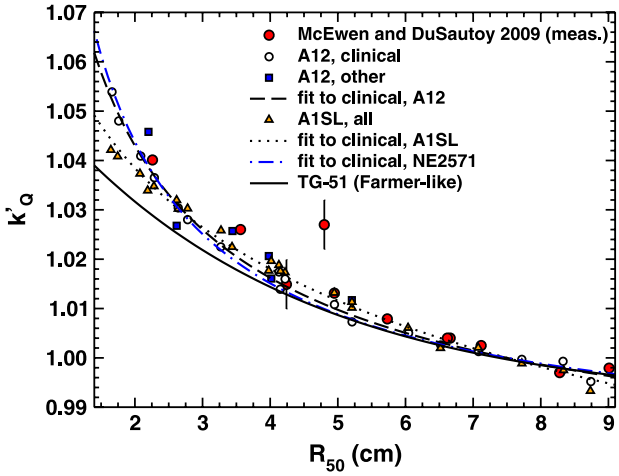

FIG. 3. The $k'_Q = k_Q/k_{Q,ecal}$ calculations (without explicitly removing gradient effects and with no EPOM shift) for the Exradin A12 (identifying results using clinical accelerator source models and nonclinical accelerator models), A1SL (all beams) chambers and the NE2571 (clinical beams only) chamber. The fits to the calculated k'_Q vs R_{50} [Eq. (11)] are shown when results from only clinical beams are considered. These results are compared to the compilation of measured values from McEwen and DuSautoy (Ref. 39) (with representative error bars) and the fit provided in TG-51 (Ref. 1) for Farmer-like cylindrical chambers. It is common practice in primary standards laboratories to report k'_Q vs R_{50} without explicitly correcting for gradient effects. The TG-51 $k'_{R_{50}}$ calculations do not include gradient effects but, as discussed in the text, the method used to account for gradient effects does not affect the trend of k'_Q or $k'_{R_{50}}$ vs R_{50}.

In Fig. 3, the k'_Q calculations are shown for the Exradin A12 chamber in realistic clinical electron beam sources and in nonclinical electron beams. If only results from clinical accelerators are considered, results are very close to a fit to calculated k'_Q factors (RMSD = 0.11% for the A12 calculations). Those from less realistic source models are more scattered about the fit (including all beams increases RMSD to 0.23% for the A12 calculations) as shown previously[13] for the NE2571 chamber. The results for the smaller volume Exradin A1SL chamber are also shown on Fig. 3, again with a fit to calculated k'_Q factors as a function of R_{50}. The same source models are used for calculations with the Exradin A1SL as those for the Exradin A12 but the dependence of k'_Q or k_Q calculations on the type of beam is not as marked for the smaller Exradin A1SL. This is likely due to the smaller influence of the replacement correction factor on the Exradin A1SL results. In addition, the curvature of the k'_Q or k_Q fit is more shallow for the Exradin A1SL chamber compared to those for cylindrical chambers with larger volumes. This is in line with the results of Wang and Rogers[45] who calculated the fluence correction factor as a function of cavity radius and R_{50} and showed that it varies less as a function of energy for chambers with a smaller cavity radius.

Table VII provides fitting coefficients for cylindrical chambers for the fit to k'_Q calculations vs R_{50} of the form

$$k'_Q = a + b \times R_{50}^{-c}, \tag{11}$$

made considering k_Q factors (without using an EPOM and including gradient effects by definition), when results from

TABLE VII. Power fitting parameters for cylindrical chambers [k'_Q vs R_{50} of the form in Eq. (11)] when results are obtained using only clinical accelerator models and chambers are positioned with their central axes at d_{ref} (no EPOM).

		Power fitting parameters			
Manufacturer	Chamber	a	b	c	RMSD (%)
NE	2571	0.977	0.117	0.817	0.15
	2611	0.979	0.120	0.875	0.09
Exradin	A12	0.965	0.119	0.607	0.11
	A19	0.957	0.119	0.505	0.14
	A12S	0.937	0.136	0.378	0.13
	A18	0.352	0.711	0.046	0.11
	A1SL	0.205	0.854	0.036	0.13
PTW	30010	0.980	0.119	0.891	0.14
	30011	0.976	0.120	0.793	0.13
	30012	0.972	0.121	0.728	0.11
	30013	0.978	0.112	0.816	0.15
	31013	0.945	0.133	0.441	0.15
IBA	FC65G	0.971	0.113	0.680	0.13
	FC65P	0.973	0.110	0.692	0.14
	FC23C	0.971	0.097	0.591	0.16
	CC25	0.964	0.105	0.539	0.16
	CC13	0.926	0.129	0.279	0.10
Capintec	PR06C/G	0.972	0.122	0.729	0.14

only clinical electron beam sources are considered. The fits to the calculated data are very tight, resulting in an RMSD of less than 0.16% for all chambers investigated.

Fits to k'_Q values vs R_{50} are provided instead of $k'_{R_{50}}$ where a calculated P_{gr}^Q correction is applied and would require the application of a measured gradient correction in the clinic. When only clinical accelerator models are considered, the fits to calculated k'_Q factors are tight and little is gained from the removal of gradient effects. In addition, requiring that the clinical physicist measures a gradient correction introduces an additional step in the calibration procedure. As in our previous work,[13] using Eq. (6) we calculate shifts (not provided here) to obtain optimal gradient corrections for the cylindrical chambers investigated here that reduce the RMSD of a fit to $k_{R_{50}}$ calculations. The resulting shifts to obtain optimal P_{gr}^Q values are very small (< 0.83 mm). It may not be practical to require clinical positioning at this level of accuracy and removing the requirement of measuring a gradient correction factor in the clinical beam simplifies the calibration procedure. However, the trends of k'_Q or $k'_{R_{50}}$ values vs R_{50} are not significantly affected by the scheme used to account for gradient effects even though $k_{R_{50},ecal}$ and $k_{Q,ecal}$ calculations are affected. For the NE2571 chamber, the fit to $k'_{R_{50}}$ vs R_{50} [$k'_{R_{50}} = k_Q/(k_{R_{50},ecal}P_{gr}^Q)$] with P_{gr}^Q calculated using the optimal shift for removal of gradient effects is at most 0.2% different from the fit to k'_Q vs R_{50} ($k'_Q = k_Q/k_{Q,ecal}$). Therefore, the results of this work can still be used for future dosimetry protocol updates whether or not the recommendation to require the application of a clinically measured gradient correction is maintained.

3.E. Sensitivity of these results to ion chamber models

Several tests have been performed to investigate the sensitivity of these calculations to variations in the ion chamber models. Above, we compared these k_Q calculations for the PTW Markus to those from Zink and Wulff[12] but discrepancies on the order of 1% in low-energy beams between the two studies were observed using an early model of the Markus chamber for the calculations of this work. The main difference between the early PTW Markus chamber model of this work and that used by Zink and Wulff[12] is the radius of the air gap between the collector and the water proofing PMMA cap in the front window of the chamber. This minor difference in the ion chamber geometry produced a significant (up to 0.7%) effect on k_Q values, particularly in low-energy beams. The effect is likely due to the influence of scattered low-energy electrons from the front window combined with the small guard width of the Markus chamber. The optimal shift to determine accurate R_{50} values was 1.71 mm using the early model compared to 1.54 mm when the calculations are performed with the updated model. In addition, the model of the PTW Markus chamber used for this work includes a model of a triaxial cable in the rear wall of the chamber. Removing these metal components does not affect the k_Q calculations by more than 0.1% in beams with R_{50} values of 3.28 and 7.06 cm.

When the physical shift is used, the $k_{Q,ecal}$ factors for the two models of the IBA NACP-02 chambers with differing graphite densities in the chambers' front window are up to 0.3% different, whereas if separate optimal shifts are used, this difference is only 0.2% (see Table IV). The optimal shifts of the NACP-02 chambers are 1.13 mm if the manufacturer specified graphite density is used and 1.31 mm if a graphite density of 2.25 g/cm^3 is used, as suggested by Chin *et al.*[22] The only difference between the IBA PPC-40 and PTW Roos chambers is the thickness of the PMMA front window, which is 1.13 mm for the PTW Roos and 1.0 mm for the IBA PPC-40. The optimal shifts for accurate R_{50} determination reflect that difference, being 0.16 mm larger for the PTW Roos chamber. The $k_{Q,ecal}$ factors for these two chambers are within 0.2% of each other and k'_Q values are also within 0.2% even in very low-energy beams.

All of the plane-parallel Exradin ion chambers use stainless steel screws to fix the front window to the chamber body. Calculations of k_Q are performed for the Exradin A11 and A10 chambers without screws in the ion chamber model. For the Exradin A11 (A10) chamber, the results from the model without screws are 0.2% and 0.5% (0.3% and 0.7%) higher than those from the original model in beams with R_{50} values of 3.28 and 7.06 cm. However, for both chambers, the value of the optimal shift to minimize the variation of P_Q with depth (similar to that for accurate R_{50} determination) is not affected within 0.06 mm by the effects of screws in the chamber models in the same beams.

We previously[13] investigated the sensitivity of $k_{Q,ecal}$ calculations to variations in the NE2571 chamber model to estimate systematic uncertainties in $k_{Q,ecal}$ calculations. The radius of the air cavity and the wall thickness were individually

varied by 10% and the resulting effects on $k_{Q,\mathrm{ecal}}$ calculations were less than 0.1%. Meanwhile, if the composition of the stem was changed entirely to aluminum, the effect on $k_{Q,\mathrm{ecal}}$ was 0.2%—similar to the overall effect of the stem on $k_{Q,\mathrm{ecal}}$ calculations investigated by changing the materials of the stem to water. Similar calculations of k_Q are performed here for the IBA FC65G and Exradin A19 chambers. The effect on k_Q of changing the chamber stems to aluminum is less than 0.3% for both chambers in beams with R_{50} values of 3.28 and 7.06 cm. The effect of the water-proofing sleeve is 0.3% in the same beams, consistent with the results of Buckley and Rogers.[44]

In summary, k_Q calculations can be quite sensitive to details in the ion chamber model (see the 1% differences in low-energy beams for the PTW Markus chamber models). We believe that our ion chamber models are realistic and accurate but the sensitivity of these calculations to ion chamber models in low-energy (4–6 MeV) electron beams suggests that systematic uncertainties in calculated k_Q factors are likely larger than those obtained in high-energy electron beams[12,13] or in photon beams.[8,46]

3.F. Uncertainty associated with practical use

Current dosimetry protocols do not recommend the use of cylindrical chambers for low-energy electron beams ($E_0 < 10$ MeV). This recommendation is based on the high values of fluence correction factors[29] required for cylindrical chambers in low-energy electron beams. The fluence correction factors used at the time to determine $k_{R_{50}}$ factors could introduce high uncertainties in the calibration of low-energy electron beams.

Figure 4 shows the change in k_Q factors with respect to R_{50}, $\Delta k_Q/\Delta R_{50}$, as a function of R_{50} for the cylindrical NE2571 and Exradin A1SL chambers as well as the plane-parallel PTW Roos chamber. The limits on this plot assume an uncertainty of 0.1% in the selection of k_Q from a fit vs R_{50} (note that the RMSD of the data to the fits in Tables V and VII are ≈0.1%) and that the combined uncertainty in ion chamber positioning and determination of R_{50} can be achieved in the clinic at the 1 mm level. It appears from this perspective that the cylindrical chambers are, in fact, better for reference dosimetry of electron beams. For the NE2571 chamber, it is true that $\Delta k_Q/\Delta R_{50}$ increases dramatically in beams with $R_{50} < 3.4$ cm (≈8 MeV) although in the worst case, from an uncertainty of 1 mm, the uncertainty associated with k_Q would still only be 0.4% due to this steep gradient. However, the calculations for the smaller volume Exradin A1SL are not subject to this steep gradient at very low R_{50} values. Both chambers can be used in lower energy beams than the PTW Roos chamber (assuming the limits established for Fig. 4) because of the smaller $\Delta k_Q/\Delta R_{50}$ in these beams. This information, along with recent observations regarding the lack of short- and long-term stability of plane-parallel chambers in photon[9] and electron[14] beams, suggests that it would be more appropriate to use cylindrical chambers for all reference dosimetry applications. However, more experimental data for cylindrical chambers, especially measured k_Q factors for comparison to this work and an analysis of their measurement performance in low-energy electron beams, are required before this recommendation can be confirmed.

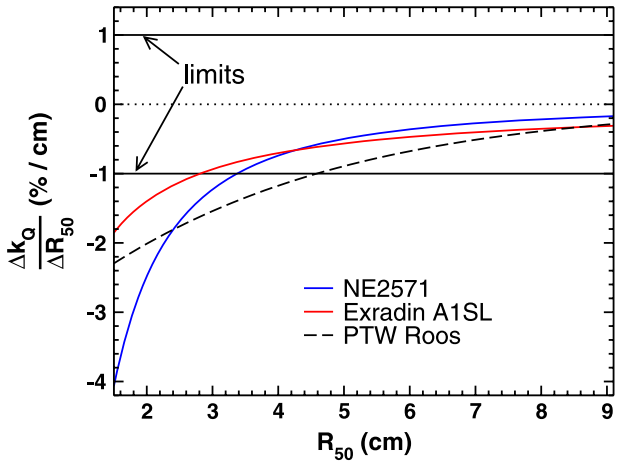

FIG. 4. The local gradient in the fit to calculated k_Q factors as a function of R_{50} for the NE2571, Exradin, A1SL and PTW Roos chambers. The limits on the useful local k_Q gradient assume a tolerance in k_Q of 0.1% and that R_{50} can be determined (including effects from chamber positioning along the beam axis) at the 1 mm level (0.1%/0.1 cm = 1%/cm).

Another potential component of uncertainty associated with positioning ion chambers in the clinic is the inherent uncertainty associated with the determination of M at the reference depth, required to measure absorbed dose to water with Eq. (1). We investigate this by calculating the % difference in $D_{\mathrm{ch}}(d_{\mathrm{ref}})$ compared to $D_{\mathrm{ch}}(d_{\mathrm{ref}} \pm 0.5$ mm) for the NE2571, Exradin A1SL and PTW Roos chambers. Using this calculated difference, we derive a type B uncertainty estimate following the JCGM Guide to the expression of uncertainty in measurement.[47] Uncertainties in $D_{\mathrm{ch}}(d_{\mathrm{ref}})$ (or the charge measured in the clinic) can be as high as 0.35% from a 0.5 mm uncertainty in positioning ion chambers. Comparing results for the NE2571, Exradin A1SL, and PTW Roos chambers, there is very little chamber dependence of the uncertainty in $D_{\mathrm{ch}}(d_{\mathrm{ref}})$ from ion chamber positioning. The spread of the calculated uncertainty values is larger in low-energy electron beams, ranging from about 0.05% to 0.35%. In high-energy beams, uncertainties in D_{ch} from chamber positioning are always less than 0.2%. These observations suggest that impacts on chamber readings from positioning can introduce uncertainties but there is little dependence of this effect on ion chamber type. Of course, this analysis assumes that all ion chamber types can be positioned with the same level of precision. It is recommended that great care be taken to position ion chambers as precisely and accurately as possible.

4. CONCLUSIONS

Combining results from all investigated beams, calculated optimal EPOM shifts are presented for 10 plane-parallel and 18 cylindrical ion chambers to accurately determine the beam quality specifier, R_{50}, from calculated values of I_{50}. An extensive comparison to literature data is performed and

the present EPOM shifts are found to be in good agreement with previously published results. For plane-parallel chambers, these shifts are also found to reduce the scatter of k_Q calculations about a fit to the data as a function of R_{50}. The optimal shifts for plane-parallel chambers determined here are different from those recommended by reference dosimetry protocols, whether the physical front window thickness or the water-equivalent front window thickness is used to determine the EPOM. For most cylindrical chambers, the optimal shifts determined here are close to 0.3 r_{cav}, smaller than the 0.5 r_{cav} shifts recommended for these chambers in reference dosimetry protocols. These results are in line with similar calculations[48,49] and measurements[50] of the shifts for cylindrical chambers in MV photon beams, which are all smaller than the 0.6 r_{cav} shift recommended in dosimetry protocols for cylindrical chambers in photon beams.

Calculations of beam quality conversion factors, k_Q or $k_{R_{50}}$, are presented and high-precision fits to the data are made. These fits are used to extract $k_{Q,\mathrm{ecal}}$ and $k_{R_{50},\mathrm{ecal}}$ factors (k_Q or $k_{R_{50}}$, depending on how gradient effects are taken into account, at $R_{50} = 7.5$ cm) which are compared to the values provided in TG-51. The largest difference between the calculated values determined here and those from TG-51 is 1.5% while the average differences (standard deviation) for plane-parallel and cylindrical chambers are 0.2% (0.6%) and 0.8% (0.5%), respectively. Differences between these values and TG-51 calculations of k_{ecal} are explained for a subset of chambers investigated using Monte Carlo calculations of individual correction factors.

After normalizing $k_{R_{50}}$ or k_Q using $k_{R_{50},\mathrm{ecal}}$ or $k_{Q,\mathrm{ecal}}$ factors to obtain $k'_{R_{50}}$ or k'_Q, the normalized energy dependence is compared to measured and calculated literature values for the subset of chambers that are most commonly used for electron beam reference dosimetry. Very good agreement is observed with other publications for the subset of plane-parallel and cylindrical chambers for which data are available. Fits to k'_Q values as a function of R_{50} [Eq. (10) plane-parallel or Eq. (11) cylindrical] are provided for each chamber. For plane-parallel chambers it is found that using an EPOM which optimizes the extraction of R_{50} also minimizes the RMSD about the fit to less than 0.15% (Table V). If only results from clinical accelerators are considered for cylindrical chambers, it is found that it is not necessary to apply an EPOM or P_{gr}^{Q} to get a fit to k'_Q values vs R_{50} with an RMSD less than 0.16% (Table VII). In both cases, the amount of scatter is less than or equal to the scatter in the fit to stopping-power ratios as a function of R_{50} used in TG-51 (see Ref. 51) and has the clear added advantage of no longer requiring the use of P_{gr}^{Q} factors in electron beams although a chamber dependent EPOM shift is required for plane-parallel chambers where none was required before.

The sensitivity of these calculations to ion chamber models is discussed. Although these calculations can be sensitive to variations in the chamber models, especially in low-energy beams, we are confident that these models are representative of realistic ion chambers.

Using the local change in the fit to k_Q with respect to R_{50} as a function of R_{50}, the uncertainty associated with the practical clinical use of these results is evaluated. We show that cylindrical chambers produce acceptable results for electron beam reference dosimetry and that smaller volume scanning ion chambers might offer the best performance due to the reduced sensitivity to electron beam source models and the smaller change in k_Q with respect to R_{50} in low-energy electron beams. Assuming that different chambers can be positioned with the same level of uncertainty, the uncertainty in the determination of absorbed dose associated with positioning ion chambers does not appear to depend on the type of ion chamber used for reference dosimetry measurements indicating that significant benefits or drawbacks are not inherent to the use of plane-parallel or cylindrical chambers at the reference depth in electron beams. However, very few measurement-based studies with cylindrical chambers in electron beams have been published and the satisfactory performance of these must be established before they can be recommended for reference dosimetry.

ACKNOWLEDGMENTS

The authors thank Malcolm McEwen of NRC for experimental work to establish the BEAMnrc model of the Elekta *Precise* Linac and useful discussions regarding practical electron beam dosimetry. The authors thank Jörg Wulff and Klemens Zink for helpful discussions regarding egs_chamber simulations and ion chamber models. Work supported by an OGSST and a NSERC CGS held by B. R. Muir, by NSERC, the CRC program, CFI and OIT.

[a]Electronic mail: Bryan.Muir@nrc-cnrc.gc.ca
[b]Electronic mail: drogers@physics.carleton.ca

[1]P. R. Almond, P. J. Biggs, B. M. Coursey, W. F. Hanson, M. S. Huq, R. Nath, and D. W. O. Rogers, "AAPM's TG-51 protocol for clinical reference dosimetry of high-energy photon and electron beams," Med. Phys. **26**, 1847–1870 (1999).
[2]IAEA, "Absorbed dose determination in external beam radiotherapy: An international code of practice for dosimetry based on standards of absorbed dose to water V12," Technical Report Series 398, http://www-naweb.iaea.org/nahu/DMRP/documents/CoP_V12_2006-06-05.pdf, 2006.
[3]L. A. Buckley and D. W. O. Rogers, "Wall correction factors, P_{wall}, for parallel-plate ionization chambers," Med. Phys. **33**, 1788–1796 (2006).
[4]J. Wulff, J. T. Heverhagen, and K. Zink, "Monte-Carlo-based perturbation and beam quality correction factors for thimble ionization chambers in high-energy photon beams," Phys. Med. Biol. **53**, 2823–2836 (2008).
[5]L. Tantot and J. P. Seuntjens, "Modelling ionization chamber response to nonstandard beam configurations," J. Phys.: Conf. Ser. **102**, 012023 (2008).
[6]D. M. González-Castaño, G. H. Hartmann, F. Sánchez-Doblado, F. Gómez, R.-P. Kapsch, J. Pena, and R. Capote, "The determination of beam quality correction factors: Monte Carlo simulations and measurements," Phys. Med. Biol. **54**, 4723–4741 (2009).
[7]M. R. McEwen, "Measurement of ionization chamber absorbed dose k_Q factors in megavoltage photon beams," Med. Phys. **37**, 2179–2193 (2010).
[8]B. R. Muir and D. W. O. Rogers, "Monte Carlo calculations of k_Q, the beam quality conversion factor," Med. Phys. **37**, 5939–5950 (2010).
[9]B. R. Muir, M. R. McEwen, and D. W. O. Rogers, "Beam quality conversion factors for parallel-plate ionization chambers in MV photon beams," Med. Phys. **39**, 1618–1631 (2012).
[10]F. Erazo and A. M. Lallena, "Calculation of beam quality correction factors for various thimble ionization chambers using the Monte Carlo code PENELOPE," Phys. Med. **29**, 163–170 (2013).
[11]K. Zink and J. Wulff, "Monte Carlo calculations of beam quality correction factors k_Q for electron dosimetry with a parallel-plate Roos chamber," Phys. Med. Biol. **53**, 1595–1607 (2008).

[12]K. Zink and J. Wulff, "Beam quality corrections for parallel-plate ion chambers in electron reference dosimetry," Phys. Med. Biol. **57**, 1831–1854 (2012).
[13]B. R. Muir and D. W. O. Rogers, "Monte Carlo calculations for reference dosimetry of electron beams with the PTW Roos and NE2571 ion chambers," Med. Phys. **40**, 121722 (16pp.) (2013).
[14]G. Bass, R. Thomas, and J. Pearce, "The calibration of parallel-plate electron ionization chambers at NPL for use with the IPEM 2003 code of practice: Summary data," Phys. Med. Biol. **54**, N115–N124 (2009).
[15]H. Svensson and A. Brahme, "Recent advances in electron and photon dosimetry," in *Radiation Dosimetry*, edited by C. G. Orton (Plenum, New York, 1986), pp. 87–170.
[16]C. D. Cojocaru and C. K. Ross, "Extracting W_{air} from the 1976 electron beam measurements of Domen and Lamperti," Med. Phys. **39**, 4645 (2012), abstract.
[17]G. X. Ding, D. W. O. Rogers, and T. R. Mackie, "Calculation of stopping-power ratios using realistic clinical electron beams," Med. Phys. **22**, 489–501 (1995).
[18]I. Kawrakow, "Accurate condensed history Monte Carlo simulation of electron transport. I. EGSnrc, the new EGS4 version," Med. Phys. **27**, 485–498 (2000).
[19]I. Kawrakow, E. Mainegra-Hing, D. W. O. Rogers, F. Tessier, and B. R. B. Walters, "The EGSnrc Code System: Monte Carlo simulation of electron and photon transport," NRC Technical Report PIRS-701 v4-2-3-2 (National Research Council Canada, Ottawa, Canada, 2011).
[20]J. Wulff, K. Zink, and I. Kawrakow, "Efficiency improvements for ion chamber calculations in high energy photon beams," Med. Phys. **35**, 1328–1336 (2008).
[21]B. R. Muir, M. R. McEwen, and D. W. O. Rogers, "Measured and Monte Carlo calculated k_Q factors: accuracy and comparison," Med. Phys. **38**, 4600–4609 (2011).
[22]E. Chin, D. Shipley, M. Bailey, J. Seuntjens, H. Palmans, A. DuSautoy, and F. Verhaegen, "Validation of a Monte Carlo model of a NACP-02 plane-parallel ionization chamber model using electron backscatter experiments," Phys. Med. Biol. **53**, N119–N126 (2008).
[23]M. R. McEwen, L. A. DeWerd, G. S. Ibbott, D. S. Followill, D. W. O. Rogers, S. M. Seltzer, and J. P. Seuntjens, "Addendum to the AAPM's TG-51 protocol for clinical reference dosimetry of high-energy photon beams," Med. Phys. **40**, 041501 (20pp.) (2013).
[24]G. Mora, A. Maio, and D. W. O. Rogers, "Monte Carlo simulation of a typical ^{60}Co therapy source," Med. Phys. **26**, 2494–2502 (1999).
[25]D. W. O. Rogers, B. Walters, and I. Kawrakow, "BEAMnrc users manual," NRC Technical Report PIRS-509(A) revL (National Research Council of Canada, Ottawa, Canada, 2011), https://www.nrc-cnrc.gc.ca/eng/solutions/advisory/beam_index.html.
[26]G. X. Ding and D. W. O. Rogers, "Energy spectra, angular spread, and dose distributions of electron beams from various accelerators used in radiotherapy," NRC Report PIRS–0439 (NRC, Ottawa, K1A 0R6, 1995).
[27]D. W. O. Rogers, B. A. Faddegon, G. X. Ding, C.-M. Ma, J. Wei, and T. R. Mackie, "BEAM: A Monte Carlo code to simulate radiotherapy treatment units," Med. Phys. **22**, 503–524 (1995).
[28]F. Lacroix, M. Guillot, M. McEwen, C. Cojocaru, L. Gingras, A. S. Beddar, and L. Beaulieu, "Extraction of depth-dependent perturbation factors for parallel-plate chambers in electron beams using a plastic scintillation detector," Med. Phys. **37**, 4331–4342 (2010).
[29]K. A. Johansson, L. O. Mattsson, L. Lindborg, and H. Svensson, "Absorbed-dose determination with ionization chambers in electron and photon beams having energies between 1 and 50 MeV," in *IAEA Symposium Proceedings,* IAEA–SM–222/35 (IAEA, Vienna, 1978), pp. 243–270.
[30]A. Van der Plaetsen, J. Seuntjens, H. Thierens, and S. Vynckier, "Verification of absorbed doses determined with thimble and parallel-plate ionization chambers in clinical electron beams using ferrous sulphate dosimetry," Med. Phys. **21**, 37–44 (1994).
[31]M. Roos, K. Derikum, and A. Krauss, "Deviation of the effective point of measurement of the Markus chamber from the front surface of its air cavity in electron beams," in *IAEA-TECDOC-1173: Review of Data and Methods Recommended in the International Code of Practice for Dosimetry IAEA Technical Reports Series No. 381, The Use of Plane Parallel Ionization Chambers in High Energy Electron and Photon Beams*, edited by IAEA (IAEA, Vienna, Austria, 2000), pp. 45–52.
[32]L. L. W. Wang and D. W. O. Rogers, "Study of the effective point of measurement for ion chambers in electron beams by Monte Carlo simulation," Med. Phys. **36**, 2034–2042 (2009).
[33]K. Zink and J. Wulff, "Positioning of a plane-parallel ionization chamber in clinical electron beams and the impact on perturbation factors," Phys. Med. Biol. **54**, 2421–2435 (2009).
[34]K. Zink and J. Wulff, "On the wall perturbation correction for a parallel-plate NACP-02 chamber in clinical electron beams," Med. Phys. **38**, 1045–1054 (2011).
[35]L. L. W. Wang and D. W. O. Rogers, "Calculation of the replacement correction factors for ion chambers in megavoltage beams by Monte Carlo simulation," Med. Phys. **35**, 1747–1755 (2008).
[36]L. L. W. Wang and D. W. O. Rogers, "Replacement correction factors for plane-parallel ion chambers in electron beams," Med. Phys. **37**, 461–465 (2010).
[37]D. W. O. Rogers, "A new approach to electron beam reference dosimetry," Med. Phys. **25**, 310–320 (1998).
[38]E. Mainegra-Hing, I. Kawrakow, and D. W. O. Rogers, "Calculations for plane-parallel ion chambers in ^{60}Co beams using the EGSnrc Monte Carlo code," Med. Phys. **30**, 179–189 (2003).
[39]M. R. McEwen and A. R. DuSautoy, "Primary standards of absorbed dose for electron beams," Metrologia **46**, S59–S79 (2009).
[40]G. Stucki and S. Voros, "Experimental $k_{Q,Q0}$ electron beam quality correction factors for the Types NACP02 and PTW34001 plane-parallel chambers," in *Proceedings of Absorbed Dose and Air Kerma Primary Standards Workshop*, LNHB, Paris, May 2007, http://www.nucleide.org/ADAKPS_WS/.
[41]F. Araki, "Monte Carlo calculations of correction factors for plane-parallel ionization chambers in clinical electron dosimetry," Med. Phys. **35**, 4033–4040 (2008).
[42]J. Sempau, P. Andreo, J. Aldana, J. Mazurier, and F. Salvat, "Electron beam quality correction factors for plane-parallel ionization chambers: Monte Carlo calculations using the PENELOPE system," Phys. Med. Biol. **49**, 4427–4444 (2004).
[43]M. R. McEwen, A. J. Williams, and A. R. DuSautoy, "Determination of absorbed dose calibration factors for therapy level electron beam ionization chambers," Phys. Med. Biol. **46**, 741–755 (2001).
[44]L. A. Buckley and D. W. O. Rogers, "Wall correction factors, P_{wall}, for thimble ionization chambers," Med. Phys. **33**, 455–464 (2006).
[45]L. L. W. Wang and D. W. O. Rogers, "Replacement correction factors for cylindrical ion chambers in electron beams," Med. Phys. **36**, 4600–4608 (2009).
[46]J. Wulff, J. T. Heverhagen, K. Zink, and I. Kawrakow, "Investigation of systematic uncertainties in Monte Carlo-calculated beam quality correction factors," Phys. Med. Biol. **55**, 4481–4493 (2010).
[47]JCGM 100:2008, Guide to the Expression of Uncertainty in Measurement (Joint Committee for Guides in Metrology, 2008).
[48]I. Kawrakow, "On the effective point of measurement in megavoltage photon beams," Med. Phys. **33**, 1829–1839 (2006).
[49]F. Tessier and I. Kawrakow, "Effective point of measurement of thimble ion chambers in megavoltage photon beams," Med. Phys. **37**, 96–107 (2010).
[50]M. R. McEwen, I. Kawrakow, and C. K. Ross, "The effective point of measurement of ionization chambers and the build-up anomaly in MV x-ray beams," Med. Phys. **35**, 950–958 (2008).
[51]D. T. Burns, G. X. Ding, and D. W. O. Rogers, "R_{50} as a beam quality specifier for selecting stopping-power ratios and reference depths for electron dosimetry," Med. Phys. **23**, 383–388 (1996).